Inorganica Chimica Acta 400 (2013) 228–238

Contents lists available at SciVerse ScienceDirect

Inorganica Chimica Acta

journal homepage: www.elsevier.com/locate/ica

Metal complexes of ditopic dithiophosphonate ligands built on a naphthalenediimide core

Radu F. Semeniuc [a,*], Robert R. Baum [a], Jedidiah J. Veach [a], Kraig A. Wheeler [a], Perry J. Pellechia [b]

[a] Department of Chemistry, Eastern Illinois University, Charleston, IL 61920, USA
[b] Department of Chemistry and Biochemistry, University of South Carolina, Columbia, SC 29208, USA

ARTICLE INFO

Article history:
Received 29 November 2012
Received in revised form 26 February 2013
Accepted 26 February 2013
Available online 7 March 2013

Dedicated to the memory of Professor Ioan Silaghi-Dumitrescu

Keywords:
Supramolecular chemistry
X-ray crystal structures
Phosphor-1,1-dithiolates
Tin complexes
Copper complexes

ABSTRACT

Ditopic ligands consisting of two dithiophosphonate donor groups attached to a 1,4,5,8-naphthalenediimide core through ether spacers of different length have been synthesized and characterized. The NDI[$(CH_2CH_2O)_n$(An)PS_2NH_4]$_2$ ligands (n = 1: **1a-[NH$_4$]$_2$**; n = 2: **1b-[NH$_4$]$_2$**; NDI = naphthalenediimide; An = anisole) react with Ph_3SnCl and $(Ph_3P)_2CuNO_3$ in a 1:2 ratio to yield bimetallic complexes (**1a-[SnPh$_3$]$_2$** and **1a-[Cu(PPh$_3$)$_2$]$_2$** for n = 1, and **1b-[SnPh$_3$]$_2$** and **1b-[Cu(PPh$_3$)$_2$]$_2$** for n = 2), and with Ph_2SnCl_2 in a 1:1 ratio to form bimetallic (**{1a-[SnPh$_2$]}$_2$**) and monometallic (**1b-[SnPh$_2$]**) macrocycles. Structural characterization of these compounds revealed monodentate and anisobidentate coordination modes of the dithiophosphonate group, as well as the presence of metal-sulfur secondary bonds. While the ditopic nature of the ligand does not have an influence over the coordination behavior of the individual –PS_2 groups, the length of the naphthalenediimide-dithiophosphonate linker lead to different solid-state supramolecular architectures. Cooperative π–π stacking and C–H···π interactions organize the supramolecular structures of these complexes, generating two-dimensional sheets (in the case of "short-arm" ligand: **1a-[SnPh$_3$]$_2$** and **1a-[Cu(PPh$_3$)$_2$]$_2$**) and mono-dimensional chains (in the case of "long-arm" ligand: **1b-[SnPh$_3$]$_2$**). In the case of **{1a-[SnPh$_2$]}$_2$** and **1b-[SnPh$_2$]** metallacycles, π–π stacking interactions between NDI central moieties produce infinite π–π stacked chains and discrete dimers, respectively.

1. Introduction

Investigations into the architecture of supramolecular metal complexes formed by self-assembly processes have been undergoing since the early 1990s. By using carefully designed polytopic ligands in combination with metallic centers having specific stereochemical requirements, interesting and unusual molecular architectures have been prepared and characterized [1–4]. Most research in this area is based on oligopyridine [1] and oligocatecholate [2] ligands, although alkynyl- [3] and pyrazolyl-based [4] ligands are also heavily employed in the synthesis of metal-directed self-assembly of supramolecular architectures.

The incorporation of the soft 1,1-dithiolate donor set [5] into polyfunctional systems represents a promising research field that has not been yet exploited to its full potential. Only recently the Beer group used the dithiocarbamate donor set to prepare supramolecular architectures such as macrocycles, cages, catenanes, and resorcinarene-based assemblies [6]. Wilton-Ely prepared piperazine-based ditopic dithiocarbamate ligands and used them in the preparation of homo- and hetero polymetallic species [7]. Polytopic dithiocarbamates were also used in the synthesis of diorganotin-based cavitands and capsules [8].

Phosphor-1,1-dithiolates represent an important group of the more general 1,1-dithiolate class of ligands, and include dithiophosphates $[(RO)_2PS_2]^-$, dithiophosphinates $[R_2PS_2]^-$, and dithiophosphonates $[(RO)R'PS_2]^-$. Usually, these ligands can coordinate to metal atoms (Scheme 1) in a monodentate (a), isobidentate (b), or anisobidentate (c) fashion. In some cases, bimetallic biconnective (d), and bimetallic triconnective (e) bridging modes were observed. In rare cases, phosphor-1,1-dithiolate ligands can bridge two metal atoms through only one sulfur atom (f) and, in the case of Cu(I) cluster compounds, the trimetallic triconnective (g) and tetrametallic tetraconnective (h) coordination modes were also described [5a,b]. This rich coordination behavior stems from the presence of soft Lewis acidic centers on these ligands, *i.e.* sulfur, thus opening the possibility of supramolecular association in the crystalline phase through secondary bonds.

Considering their well-documented and varied coordination modes, as well as their availability, it is surprising that reports of ditopic phosphor-1,1-dithiolates are extremely scarce. The dithiophosphonato ligand is the least studied member of the phosphor-1,1-dithiolate family. While reports of their use (in combination with pyridine-based ligands) in the synthesis of metal-directed

* Corresponding author. Tel.: +1 217 581 5422.
E-mail address: rsemeniuc@eiu.edu (R.F. Semeniuc).

0020-1693/$ - see front matter © 2013 Elsevier B.V. All rights reserved.
http://dx.doi.org/10.1016/j.ica.2013.02.037

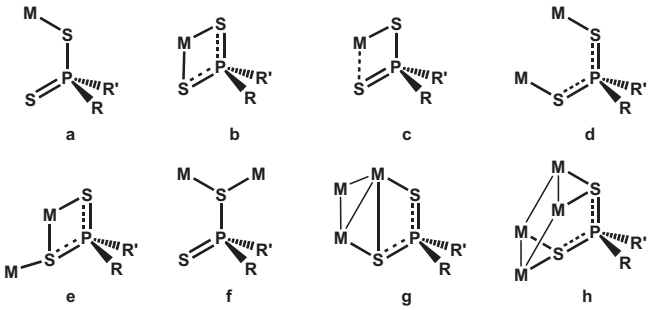

Scheme 1. Coordination modes of phosphor-1,1-dithiolate ligands.

self-assembly of supramolecular architectures are known [9], to date there are no significant studies on the synthesis of polytopic dithiophosphonates and their use in coordination and supramolecular chemistry [10].

We report here the preparation of ditopic ligands consisting of two dithiophosphonate donor groups attached to a 1,4,5,8-naphthalenediimide core through ether spacers of different length and the reactions of these ligands with metallic centers to form discrete coordination compounds. Their molecular and supramolecular structures and solution behavior are also discussed.

2. Results and discussion

2.1. Synthesis and general characteristics of the ligands and their complexes

The ditopic dithiophosphonate ligands were synthesized (Scheme 2) by the reaction of 1,4,5,8-naphthalenetetracarboxylic dianhydride with two equivalents of either 2-aminoethanol or 2-(2-aminoethoxy)ethanol in ethanol, followed by the reaction of the resulting naphthalenediimide (**NDI**) based diols with the commercially available 1,3,2,4-dithiadiphosphetane-2,4-bis(4-methoxy-phenyl)-2,4-disulfide (Lawesson's Reagent, L. R.) in refluxing benzene. The ammonium salts NDI-$[(CH_2CH_2O)_n(An)\text{-}PS_2NH_4]_2$ ($n = 1$: **1a-[NH_4]$_2$**; $n = 2$: **1b-[NH_4]$_2$**; An = anisole) were then precipitated by passing a stream of dry gaseous NH_3 through the cold benzene solution of the dithiophosphonic acids. The ligands were isolated in good yields as air and moisture stable orange powders, soluble in water and alcohols and insoluble in other common organic solvents.

The metathesis reaction of these ditopic dithiophosphonates and Ph_3SnCl or $(Ph_3P)_2CuNO_3$ in a 1:2 ratio yielded the bimetallic compounds **1a-[SnPh$_3$]$_2$** and **1a-[Cu(PPh$_3$)$_2$]$_2$** for $n = 1$, and **1b-[SnPh$_3$]$_2$** and **1b-[Cu(PPh$_3$)$_2$]$_2$** for $n = 2$, in moderate to good yields, Scheme 3, top. The reactions proceed easily in a CH_2Cl_2/H_2O biphasic setting and the completion of the reaction is indicated by the loss of the color of the aqueous phase and the appearance of an orange color in the organic phase. The same reaction performed in the presence of one equivalent of Ph_2SnCl_2 afforded the bimetallic **{1a-[SnPh$_2$]}$_2$** and monometallic **1b-[SnPh$_2$]** macrocyclic compounds, respectively, see Scheme 3 middle and bottom. The compounds are orange solids, stable in air and in the presence of moisture, soluble in chlorinated solvents and only sparingly soluble in other organic solvents, such as acetone and acetonitrile.

Elemental analyses confirmed the bimetallic composition of **1a** and **1b** type of compounds, as well as of the **{1a-[SnPh$_2$]}$_2$** metallacycle, and the presence of only one metallic center in the case of

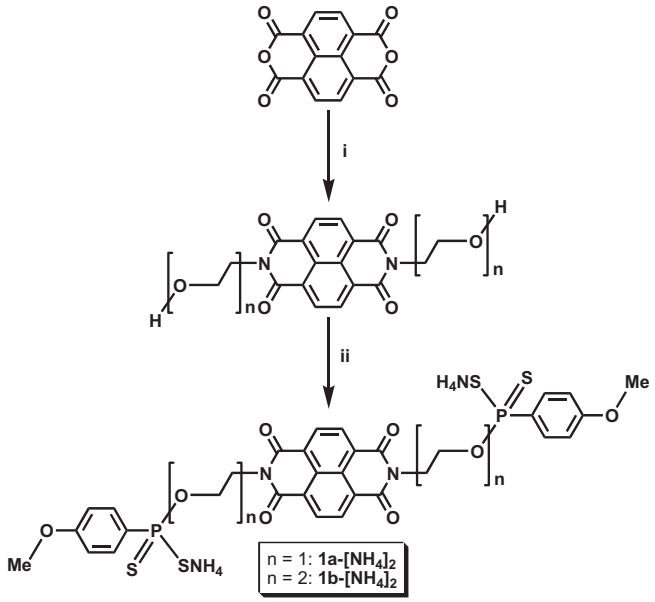

Scheme 2. Synthetic pathway toward the ditopic dithiophosphonate ligands: (i) $H_2N(CH_2CH_2O)_nOH$ ($n = 1$, 2), EtOH, reflux overnight; (ii) Lawesson's Reagent, benzene, reflux 2 h., then dry, gaseous NH_3.

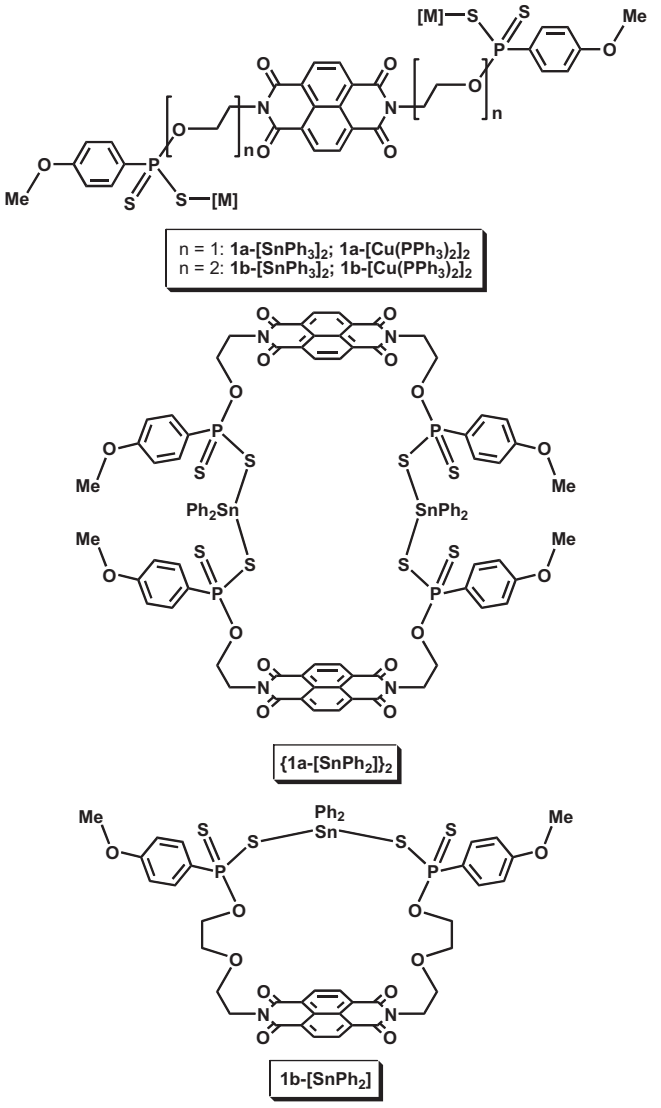

Scheme 3. Descriptive structures of the metal complexes described in this work; [M] = $SnPh_3$ and $Cu(PPh_3)_2$.

1b-[$SnPh_2$]. The sharp and well defined peaks in the ^{1}H NMR spectra of **{1a-[$SnPh_2$]}$_2$** and **1b-[$SnPh_2$]** suggests the presence of discrete assemblies in solution, as opposed to mixtures of oligo- and/or polymeric species, which usually show broad peaks. [1g–i] An NMR comparative analysis of the free ligands with the metal complexes described here was precluded by the difference in the solubility of these compounds: while the ligands are soluble in water and alcohols, the complexes show no solubility in these solvents.

2.2. Crystallographic studies

Crystals suitable for X-ray diffraction studies were grown using the layering technique: in a 15 cm test tube, approximately 50 mg of each compound were dissolved in 20 mL CH_2Cl_2 and the solution was carefully layered with about 80 mL hexanes. After several days at room temperature single crystals of **1a-[$SnPh_3$]$_2$**, **1a-[Cu(PPh_3)$_2$]$_2$**, **1b-[$SnPh_3$]$_2$**, **{1a-[$SnPh_2$]}$_2$**, and **1b-[$SnPh_2$]** were obtained. Crystallographic details for these compounds are summarized in Table 1.

2.2.1. Molecular and crystal structure of *1a-[$SnPh_3$]$_2$*

The asymmetric unit consists of half of a **1a-[$SnPh_3$]$_2$** molecule situated about an inversion center. The molecular structure of **1a-[$SnPh_3$]$_2$**, together with selected bond lengths and angles, is shown in Fig. 1, and consists of two –(An)PS_2 moieties coordinated to two -$SnPh_3$ metallic centers in a monodentate fashion (Scheme 1a).

The overall geometry around the Sn(IV) center is distorted tetrahedral, with three practically equal carbon-tin bonds (Sn–C average 2.164 Å) and with one Sn–S bond of 2.450(4) Å. The second sulfur atom of the dithiophosphonate group is also oriented toward the Sn center. The Sn–S(1) separation of 3.7 Å is too long to be considered a covalent bond, but is shorter than the sum of the van der Waals radii of tin and sulfur atoms (3.97 Å) [11]. As such, this interaction is best described as a secondary bond (dashed line in Fig. 1) [12]. An important structural feature of **1a-[$SnPh_3$]$_2$** is the *trans* orientation of the –(An)PS_2SnPh_3 groups with respect to the central **NDI** moiety. The short –CH_2CH_2O– linker place the two metallic regions in close proximity, with the –$SnPh_3$ group on top and below the naphthalenediimide plane. This orientation is only a consequence of the length of the linker and is not supported by any non-covalent interactions between the phenyl rings and **NDI**.

The crystal packing of **1a-[$SnPh_3$]$_2$** is based on a combination of π–π stacking [13] and C–H···π interactions [14] (Fig. 2). A phenyl ring from one molecule (pictured in blue) is stacked above the **NDI** core from a neighboring (orange) molecule, with a perpendic-

Table 1
Crystal data and structure refinement for **1a-[$SnPh_3$]$_2$**, **1a-[Cu(PPh_3)$_2$]$_2$**, **1b-[$SnPh_3$]$_2$**, **{1a-[$SnPh_2$]}$_2$**, and **1b-[$SnPh_2$]**.

	1a-[$SnPh_3$]$_2$	1a-[Cu(PPh_3)$_2$]$_2$	1b-[$SnPh_3$]$_2$	{1a-[$SnPh_2$]}$_2$	1b-[$SnPh_2$]
Formula	$C_{68}H_{56}N_2O_8P_2S_4Sn_2$	$C_{104}H_{86}Cu_2N_2O_8P_6S_4{\cdot}2(CH_2Cl_2)$	$C_{72}H_{64}N_2O_{10}P_2S_4Sn_2$	$C_{88}H_{72}N_4O_{16}P_4S_8Sn_2{\cdot}2(CH_2Cl_2)$	$C_{48}H_{44}N_2O_{10}P_2S_4Sn{\cdot}2(CH_2Cl_2)$
Formula weight (g mol^{-1})	1456.79	2102.74	1544.81	2229.21	1287.57
Crystal system	triclinic	triclinic	monoclinic	triclinic	triclinic
a (Å)	9.1471(11)	9.2045(1)	13.7321(2)	10.9684(2)	12.3562(3)
b (Å)	13.3620(15)	11.5410(2)	10.5102(2)	12.3642(2)	13.0479(2)
c (Å)	14.7072(17)	23.4034(4)	23.2601(3)	17.6112(3)	18.2453(4)
α (°)	75.808(5)	85.150(1)	90.00	87.540(1)	91.4050(10)
β (°)	78.661(5)	89.605(1)	97.7400(10)	88.133(1)	105.8360(10)
γ (°)	87.864(5)	75.421(1)	90.00	71.074(1)	105.2590(10)
Z	1	1	2	1	2
V (Å)	1708.6(3)	2397.19(6)	3326.48(9)	2256.71(7)	2715.40(10)
T (K)	100(2)	173(2)	100(2)	100(2)	100(2)
Space group	*P*1	*P*1	*Pc*	*P*1	*P*1
R_1 [$I > 2\sigma(I)$]	0.0990	0.0408	0.0371	0.0268	0.0450
wR_1 [$I > 2\sigma(I)$]	0.2289	0.0975	0.0881	0.0714	0.1182

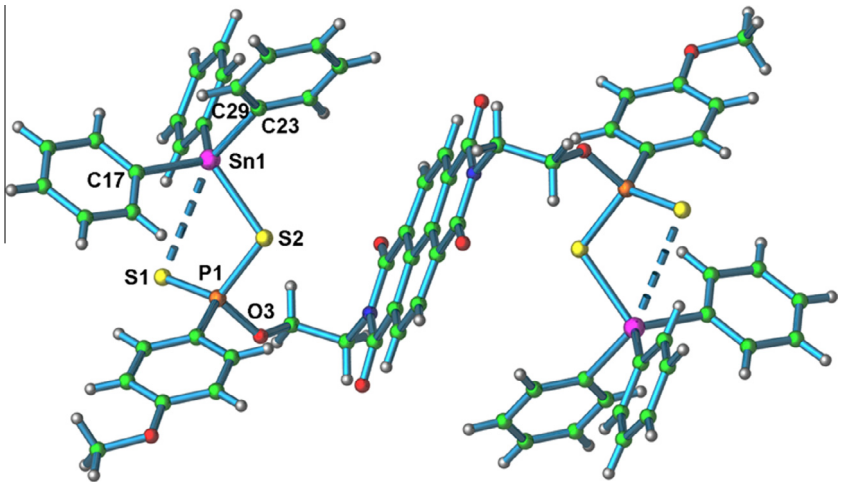

Fig. 1. Molecular structure of **1a-[$SnPh_3$]$_2$**; selected bond lengths (Å) and angles (°): Sn1–S2 = 2.450(4); Sn1–C17 = 2.175(16); Sn1–C23 = 2.172(13); Sn1–C29 = 2.145(17); S1–P1 = 1.938(7); S2–P1 = 2.080(4); P1–O3 = 1.587(12); P1–C10 = 1.772(15); S2–Sn1–C17 = 109.4(4); S2–Sn1–C23 = 97.8(4); S2–Sn1–C29 = 116.0(4); Sn1–S2–P1 = 105.12(19); S1–P1–S2 = 115.2(2); color code: carbon-green; hydrogen-gray; phosphorus-orange; sulfur-yellow; tin-purple. (For interpretation of the references to color in this figure legend, the reader is referred to the web version of this article.)

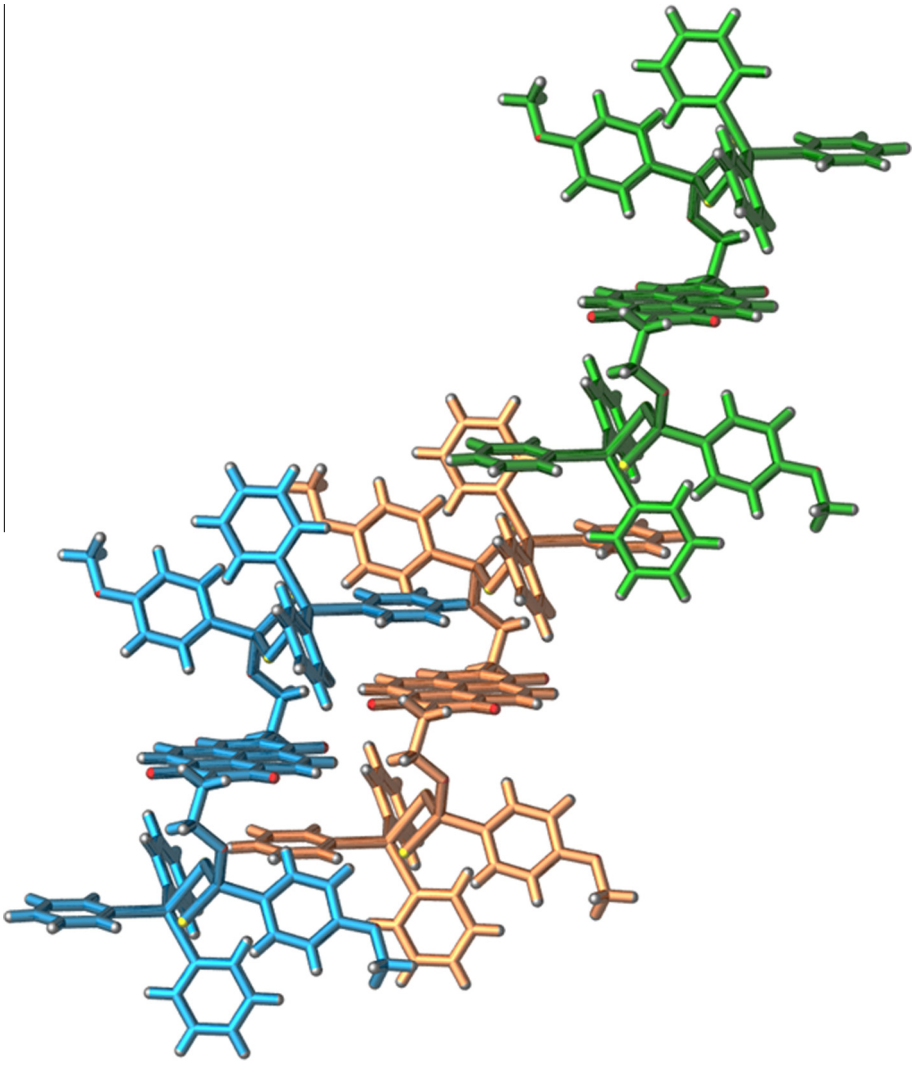

Fig. 2. Crystal packing of **1a-[SnPh$_3$]$_2$**: the phenyl-**NDI** π–π stacking interactions are shown between the blue and orange molecules and the sextuple phenyl embraces between the orange and green molecules. (For interpretation of the references to color in this figure legend, the reader is referred to the web version of this article.)

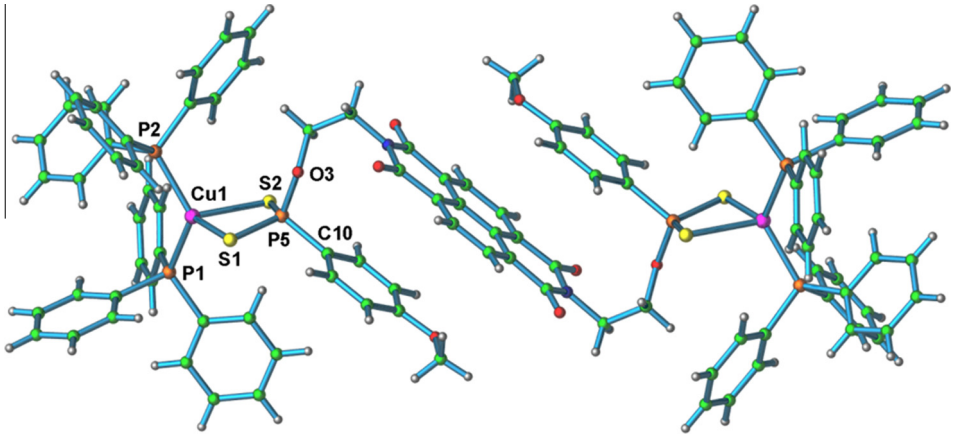

Fig. 3. Molecular structure of **1a-[Cu(PPh$_3$)$_2$]$_2$**; selected bond lengths (Å) and angles (°): Cu1–S1 = 2.386(9); Cu1–S2 = 2.548(4); Cu1–P1 = 2.267(7); Cu1–P2 = 2.271(5); S1–P5 = 1.995(8); S2–P5 = 1.985(0); P5–O3 = 1.614(9); P5–C10 = 1.808(0); S1–Cu1–S2 = 85.30; P1–Cu1–P2 = 124.12; S1–Cu1–P1 = 114.62; S1–Cu1–P2 = 112.69; S2–Cu1–P1 = 101.19; S2–Cu1–P2 = 110.69; S1–P5–S2 = 114.39; O3–P5–C10 = 103.53; color code: carbon-green; hydrogen-gray; phosphorus-orange; sulfur-yellow; copper-purple. (For interpretation of the references to color in this figure legend, the reader is referred to the web version of this article.)

ular distance between the rings of 3.5 Å. In a separate interaction, each –SnPh$_3$ group is involved in sextuple phenyl embraces [15] with another molecule, as shown for the orange and green units. This collection of interactions generates a bi-dimensional

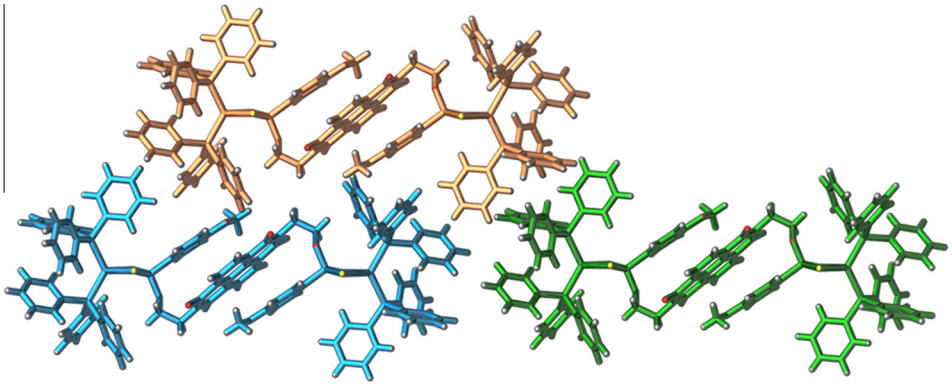

Fig. 4. Crystal packing of **1a-[Cu(**PPh_3**)$_2$]$_2$**: the sextuple phenyl embraces are pictured between the orange and green molecules; the blue unit interacts with both green and orange molecules *via* C–H···π interactions. (For interpretation of the references to colour in this figure legend, the reader is referred to the web version of this article.)

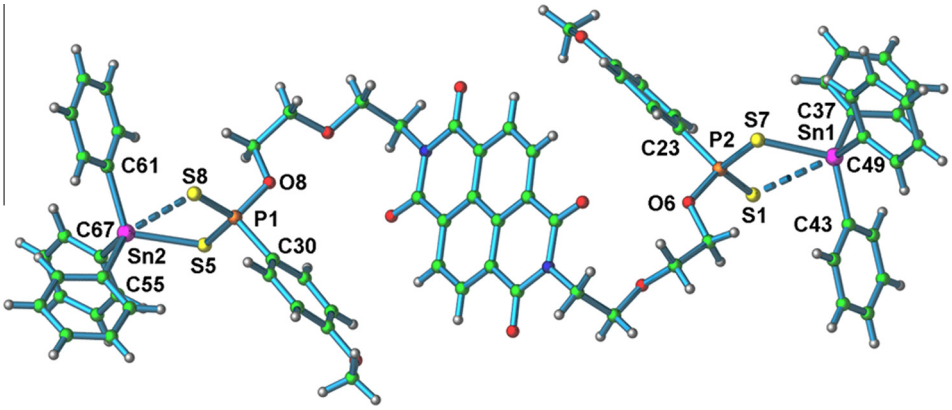

Fig. 5. Molecular structure of **1b-[SnPh$_3$]$_2$**; selected bond lengths (Å) and angles (°): Sn1–S7 = 2.440(2); Sn1–C37 = 2.109(8); Sn1–C43 = 2.113(6); Sn1–C49 = 2.143(7); Sn2–S5 = 2.4326(17); Sn2–C55 = 2.138(7); Sn2–C61 = 2.123(6); Sn2–C67 = 2.156(7); S1–P2 = 1.929(3); S7–P2 = 2.077(2); S5–P1 = 2.085(2); S8–P1 = 1.934(2); P1–O8 = 1.597(5); P1–C30 = 1.804(7); P2–O6 = 1.594(5); P2–C23 = 1.784(7); S7–Sn1–C37 = 109.0(2); S7–Sn1–C43 = 116.24(19); S7–Sn1–C49 = 96.0(2); Sn1–S7–P2 = 103.92(9); S1–P2–S7 = 115.45(11); O6–P2–C23 = 99.9(3); S5–Sn2–C55 = 110.8(2); S5–Sn2–C61 = 115.78(19); S5–Sn2–C67 = 97.1(2); Sn2–S5–P1 = 102.22(8); S5–P1–S8 = 114.79(11); O8–P1–C30 = 100.4(3); color code: carbon-green; hydrogen-gray; phosphorus-orange; sulfur-yellow; tin-purple. (For interpretation of the references to color in this figure legend, the reader is referred to the web version of this article.)

supramolecular network running along the diagonal of the unit cell.

2.2.2. Molecular and crystal structure of ***1a-[Cu(PPh$_3$)$_2$]$_2$***

The molecular structure of **1a-[Cu(**PPh_3**)$_2$]$_2$** (Fig. 3) consists of two –(An)PS_2 moieties coordinated to two -Cu(PPh_3)$_2$ metallic centers in an anisobidentate fashion (Scheme 1c), with the Cu(1)–S(1) and Cu(1)–S(2) distances of 2.386(9) and 2.548(4) Å respectively. The 0.162 Å difference between the two bond lengths is indicative of an anisobidentate coordination mode (Scheme 1c) of the dithiophosphonate ligand. In related isobidentate (Ph_3P)$_2$Cu compounds [5], the copper(I)–sulfur distances are practically equal, with a difference between the Cu–S bonds less than 0.015 Å. The geometry about the copper(I) ion is distorted tetrahedral, with the large distortions arising from the restricted "bite" angle of the dithiophosphonate ligand, the S(1)–Cu(1)–S(2) and P(1)–Cu(1)–P(2) angles being 85.30° and 124.12° respectively. As with **1a-[SnPh$_3$]$_2$**, the compound adopts a *trans* orientation with respect to the central **NDI** group and the short –CH_2CH_2O– linker place the –(An)PS_2(CuPPh_3)$_2$ group close to the core of the ligand. In contrast to **1a-[SnPh$_3$]$_2$** where no interactions were found between the metallic termini and the **NDI** group, in **1a-[Cu(**PPh_3**)$_2$]$_2$** the anisole groups are involved in intermolecular π–π stacking interactions with the aromatic core, several $C_{Anisole}$– C_{NDI} distances being between 3.4 and 3.6 Å.

The crystal packing of **1a-[Cu(**PPh_3**)$_2$]$_2$** is driven by a similar collection of π–π stacking and C–H···π interactions involving both –PPh_3 groups coordinated to the Cu(I) atom (Fig. 4). Each end of every molecule is involved in sextuple phenyl embraces, shown in Fig. 4 between the orange and green units. In addition, a third molecule (blue) interacts *via* C–H···π interactions with both orange and green neighbors, thus generating sheets in the *bc* plane of the unit cell.

2.2.3. Molecular and crystal structure of ***1b-[SnPh$_3$]$_2$***

The asymmetric unit of this compound consists of an entire **1b-[SnPh$_3$]$_2$** molecule. As with its "shorter" counterpart **1a-[SnPh$_3$]$_2$**, the molecular structure of **1b-[SnPh$_3$]$_2$** comprises of two (An)PS_2 moieties coordinated to two -$SnPh_3$ metallic centers in a monodentate fashion, see Fig. 5. The geometric parameters around the tin atoms are virtually the same as in the case of **1a-[SnPh$_3$]$_2$**, showing that the coordination behavior of the –(An)PS_2 moieties is independent of the length of the side arms attached to the naphthalenediimide group. The overall geometry around the Sn(IV) centers is distorted tetrahedral. The Sn(1)–S(7) and Sn(2)–S(5) distances are 2.440(2) and 2.4326(17) Å, respectively. The secondary interactions between the second sulfur atoms of the dithiophosphonate donor sets and tin centers are 3.46 and 3.55 Å, respectively, and are pictured as dashed lines in Fig. 5. The different relative orientation of the **NDI** and –(An)PS_2SnPh_3 regions (when compared to **1a-[SnPh$_3$]$_2$**) is driven by the different length of the ether link of the ligand: the longer side-arm place the metal-containing moieties away from the center of the ligand, to the left and right sides of the **NDI** plane.

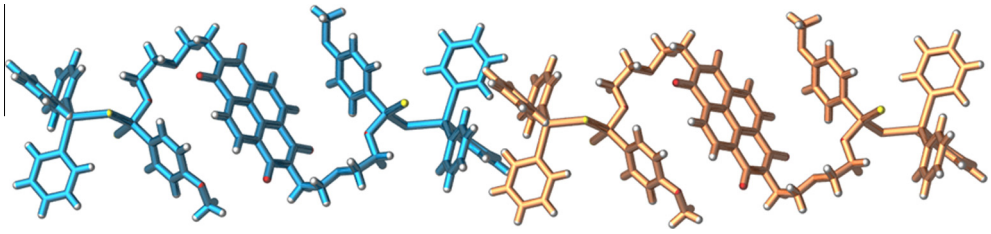

Fig. 6. Crystal packing of **1b-[$SnPh_3$]$_2$** supported by sextuple phenyl embraces.

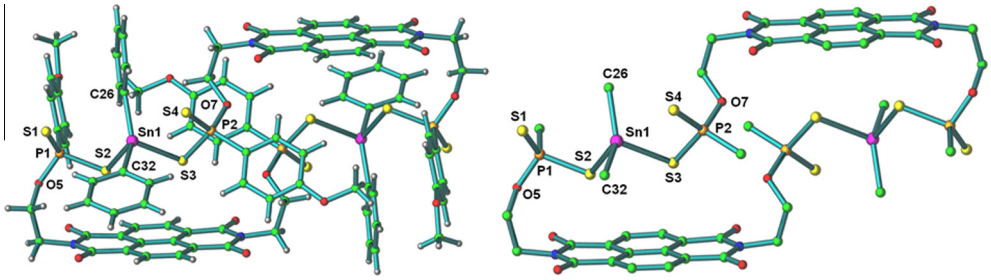

Fig. 7. Molecular structure of **{1a-[$SnPh_2$]}$_2$**: left – the complete structural features; right – hydrogen atoms and phenyl groups removed for clarity; selected bond lengths (Å) and angles (°): Sn1–C26 = 2.135(2); Sn1–C32 = 2.136(3); Sn1–S3 = 2.4996(6); Sn1–S2 = 2.5111(6); S1–P1 = 1.9370(9); S2–P1 = 2.0629(8); S3–P2 = 2.0507(9); S4–P2 = 1.9703(9); P1–O5 = 1.6089(17); P1–C19 = 1.794(3); P2–O7 = 1.5909(18); P2–C38 = 1.792(3); C26–Sn1–C32 = 139.28(9); C26–Sn1–S3 = 109.11(7); C32–Sn1–S3 = 106.16(7); C26–Sn1–S2 = 101.49(7); C32–Sn1–S2 = 101.74(7); S3–Sn1–S2 = 84.113(19); color code: carbon-green; hydrogen-gray; phosphorus-orange; sulfur-yellow; tin-purple. (For interpretation of the references to color in this figure legend, the reader is referred to the web version of this article.)

The supramolecular structure of **1b-[$SnPh_3$]$_2$** is supported only by sextuple phenyl embraces of the –$SnPh_3$ groups (the blue and orange molecules, Fig. 6). These interactions build up chains running along the diagonal of the unit cell, with the rest of the crystal packing being driven by van der Waals forces. Importantly, the **NDI** moiety is not involved in any supramolecular interaction, being "protected" by the position of the anisole groups, see Figs. 5 and 6.

*2.2.4. Molecular and crystal structure of **{1a-[$SnPh_2$]}$_2$***

The asymmetric unit consists of half of a **{1a-[$SnPh_2$]}$_2$** molecule situated about an inversion center. The molecular structure of **{1a-[$SnPh_2$]}$_2$**, together with selected bond lengths and angles, is shown in Fig. 7, and consists of two NDI-[CH_2CH_2O(An)PS_2^- ligands coordinated to two Ph_2Sn metallic centers, with the formation of a bimetallic 38-member macrocycle. The overall primary geometry around the Sn(IV) center is again distorted tetrahedral, with two equal Sn–C (2.135 Å) and Sn–S (2.505 Å) bonds. The other sulfur atoms of the two dithiophosphonate groups are also oriented toward the Sn center. However, there is a significant difference between these S–Sn distances: while the S(1)–Sn(1) distance of 3.648 Å is indicative of a secondary sulfur-tin interaction, the S(4)–Sn(1) distance of 2.980 Å suggests an anizobidentate coordination of the PS_2^- donor set to the tin center. Taking in consideration these non-covalent interactions, the geometry around the tin atom can be described as highly distorted octahedral.

The **NDI** cores of the macrocycles are involved in π–π stacking interactions, with a perpendicular distance between the rings of 3.3 Å, with several C–C distances around 3.4 Å. The rings are parallel (dihedral angle $\alpha = 0.0°$) and in an offset arrangement, with a slip angle β of 22.9°. These interactions built up π-stacked chains, shown in Fig. 8.

*2.2.5. Molecular and crystal structure of **1b-[$SnPh_2$]***

The asymmetric unit of this compound consists of an entire **1b-[$SnPh_2$]** molecule. The molecular structure of **1b-[$SnPh_2$]**, together with selected bond lengths and angles, is shown in Fig. 9, and consists of one dithiophosphonate ligand coordinated to one Sn(IV) center, with the formation of a 25-member macrocycle. As with **{1a-[$SnPh_2$]}$_2$** above, the overall primary geometry around the tin atom is distorted tetrahedral, with two practically equal Sn–C (2.115 and 2.130 Å) and Sn–S (2.473 and 2.490 Å) bonds. In contrast to **{1a-[$SnPh_2$]}$_2$** above, the other sulfur atoms of the dithiophosphonate group are situated at similar distances (3.175 and 3.285 Å), both suggesting secondary sulfur-tin interactions, and making the geometry around the tin atom distorted octahedral.

As with **{1a-[$SnPh_2$]}$_2$**, the supramolecular structure of **1b-[$SnPh_2$]** is driven by the π–π stacking of the **NDI** regions of the macrocycle. The perpendicular distance between the **NDI** rings is 3.4 Å, with several C–C distances around 3.5 Å. The rings are again parallel (dihedral angle $\alpha = 0.0°$) and in an offset arrangement, with a slip angle β of 33.2°. However, these interactions built up only dimers (see Fig. 10), due to the fact that there is only one **NDI** group present within the structure of each **1b-[$SnPh_2$]** macrocycle.

2.3. Solution studies

2.3.1. UV–Vis and fluorescence studies

Photophysical experiments were conducted at 293 K in H_2O solution for the anionic ligands and CH_2Cl_2 solution for the rest of the compounds. The results are summarized in Table 2 and presented in Fig. 11.

The absorption spectra of the compounds show no significant changes upon coordination of the ligands to the metallic centers. Tin-based compounds undergo a decrease in absorption intensity relative to their parent ligands, while the copper-based compounds show an increase in absorption intensity.

Upon excitation at $\lambda_{ex} = 345$ nm, all compounds exhibit a structured fluorescence band (around 390 and 408 nm, see Table 2), originating from the **NDI** core of the compounds, that can be assigned to a π–π^* transition [16]. Again, the coordination of the **1a** and **1b** ligands to the tin and copper centers does not cause significant changes in the emission properties of the **NDI** core.

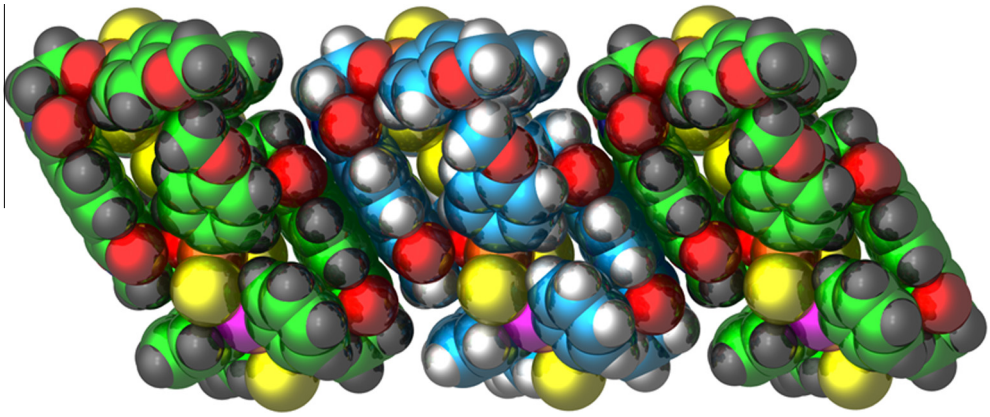

Fig. 8. Space filling representation of three π–π stacked macrocycles of **{1a-[SnPh$_2$]}$_2$**; the different colors of the macrocycles are for clarity purposes only. (For interpretation of the references to colour in this figure legend, the reader is referred to the web version of this article.)

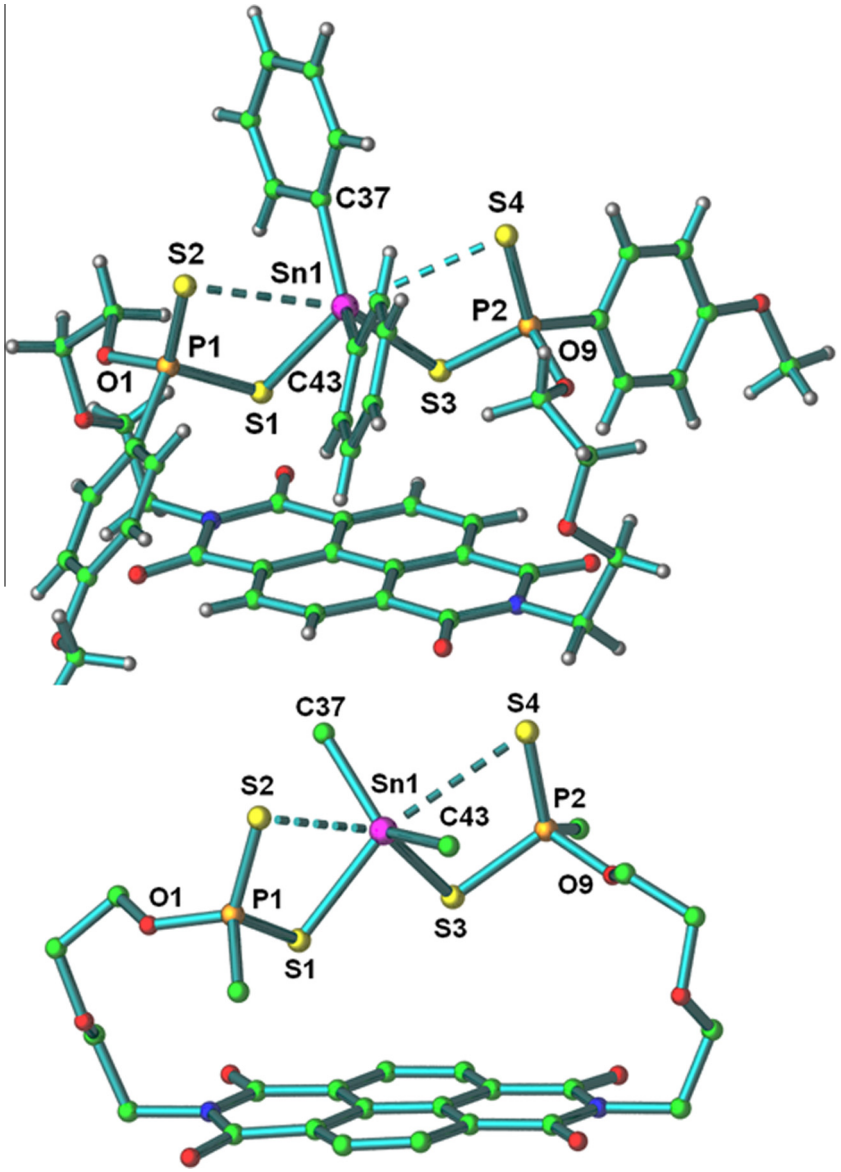

Fig. 9. Molecular structure of **1b-[SnPh$_2$]**: top – the complete structural features; bottom – hydrogen atoms and phenyl groups removed for clarity; selected bond lengths (Å) and angles (°): Sn1–C43 = 2.114(4); Sn1–C37 = 2.129(5); Sn1–S1 = 2.4730(10); Sn1–S3 = 2.4904(10); S1 P1 2.0754(14); S2–P1 = 1.9424(15); S3–P2 = 2.0608(14); S4–P2 = 1.9517(15); C43–Sn1–C37 = 127.94(18); C43–Sn1–S1 = 106.07(12); C37–Sn1–S1 = 109.09(13); C43–Sn1–S3 = 105.34(11); C37–Sn1–S3 = 115.48(13); S1–Sn1–S3 = 83.74(3); S1–Sn1–S3 = 83.74(3); color code: carbon-green; hydrogen-gray; phosphorus-orange; sulfur-yellow; tin-purple. (For interpretation of the references to color in this figure legend, the reader is referred to the web version of this article.)

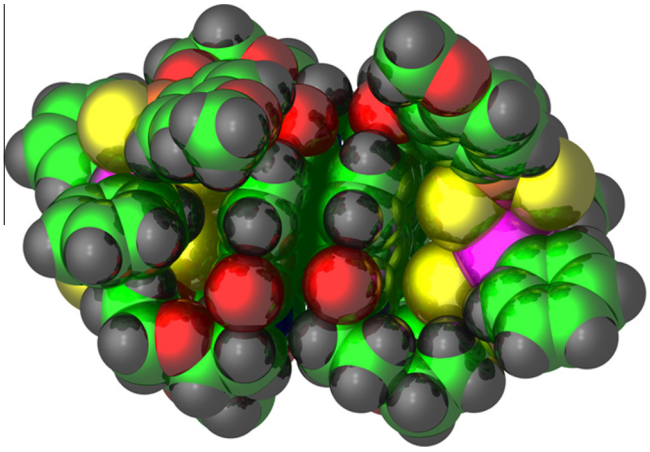

Fig. 10. Space filling representation of two π–π stacked macrocycles **1b-[SnPh$_2$]**.

Table 2
Absorption and emission data for **1a-[**NH_4**]$_2$**, **1b-[NH_4]$_2$**, **1a-[$SnPh_3$]$_2$**, **1a-[$Cu(PPh_3)_2$]$_2$**, **1b-[$SnPh_3$]$_2$**, **1b-[$Cu(PPh_3)_2$]$_2$**, **{1a-[$SnPh_2$]}$_2$**, and **1b-[$SnPh_2$]**.

	Absorption (λ_{max}/nm) (ε/$M^{-1}cm^{-1}$)	Emission (λ_{em}/nm)
1a-[NH_4]$_2$	384 (1443); 365 (1333); 345 (838)	389, 411
1b-[NH_4]$_2$	384 (1468); 364 (1355); 345, sh (873)	392, 433
1a-[$SnPh_3$]$_2$	381 (1463); 361 (1235); 342 (753)	386, 407
1a-[$Cu(PPh_3)_2$]$_2$	380 (2310); 360 (2050); 343 (1325)	388, 408
1b-[$SnPh_3$]$_2$	381 (1358); 361 (1148); 342 (690)	386, 406
1b-[$Cu(PPh_3)_2$]$_2$	381 (2828); 361 (2445); 343 (1585)	389, 407
{1a-[$SnPh_2$]}$_2$	381 (1090); 361 (960); 343 (600)	388, 410
1b-[$SnPh_2$]	381 (1010); 361 (875); 343 (543)	387, 408

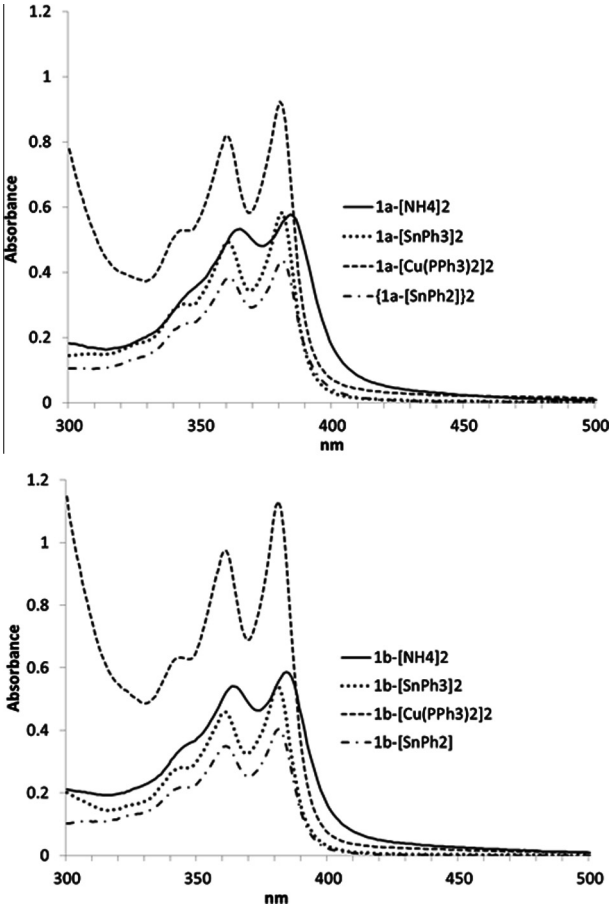

Fig. 11. Absorption spectra of **1a-[**NH_4**]$_2$** and **1b-[**NH_4**]$_2$** (H_2O), and **1a-[$SnPh_3$]$_2$**, **1a-[Cu**(PPh_3**)$_2$]$_2$**, **1b-[$SnPh_3$]$_2$**, **1b-[Cu**(PPh_3**)$_2$]$_2$**, **{1a-[$SnPh_2$]}$_2$**, and **1b-[$SnPh_2$]** (CH_2Cl_2) at 293 K.

2.3.2. NMR studies

Having observed supramolecular assemblies of these compounds in solid state, association of these complexes in solution phase was investigated by DOSY-NMR. This technique provides an indirect measure of molecular size by allowing the determination of the diffusion coefficient of a given species in solution. Subsequent application of the Stokes–Einstein equation then yields the hydrodynamic radius, r_H, which typically falls within ca. 20% of the determined crystallographic radius. This technique has been used successfully in a number of different applications, including establishing the presence or absence of dimeric species in solution [17]. Nevertheless, the above structures are not spherical, and thus a straightforward application of the Stokes–Einstein equation is precluded.

As such, we have turned our attention to Graham's law of diffusion, which relates the diffusion rate of a given species in solution at a specific temperature to its molecular mass: $D = K(T/m)^{1/2}$ (where D = diffusion rate, T = temperature, m = molecular mass, and K = a constant depending on several factors). By comparing the diffusion rate of a supramolecular species with the observed value of the solvent, and assuming that both K and T are the same for all the species present, it is possible to estimate the molecular mass of the former by applying the following equation: $MW_B = MW_A(D_A/D_B)^2$ (where MW_B = molecular weight of the species, MW_A = molecular weight of the solvent, D_A = diffusion rate of the solvent and D_B = diffusion rate of the species). While this method does not yield a precise value for the molecular mass of a species, it is accurate enough to offer the possibility to distinguish between associated and non-associated species: indeed, this method has been used to investigate the presence or absence of supramolecular association in solution in several cases [18].

In our case, the only compound showing supramolecular association in $CDCl_3$ solution is **1b-[SnPh$_2$]**. The diffusion rates retrieved from the DOSY experiment (expressed in logm^2/s) are −8.63 for $CDCl_3$ and −9.25 for **1b-[SnPh$_2$]**. Based on these values, the calculated MW of the complex is 2074.58 Daltons, very close to the theoretical value for the MW of the dimer (2235.58 Daltons), a less than 10% difference. For comparison, in the case of **{1a-[SnPh$_2$]}$_2$**, the diffusion rates are −8.63 for $CDCl_3$ and −9.27 for the macrocycle. As such, the calculated MW is 2274.74 Daltons, value which this time falls very close (again with a difference of about 10%) to the theoretical value for the non-associated species, 2059.37 Daltons. These results suggest that the asymmetric nature of **1b-[SnPh$_2$]** (only one **NDI** group, as opposed to two **NDI** moieties in the case of **{1a-[SnPh$_2$]}$_2$**) might be responsible for the observed association of these molecular species in solution. DOSY-NMR data also suggest that while the phenyl embraces interactions are capable to support supramolecular associations of the remaining bimetallic **1a** and **1b** compounds in the solid state, they are not strong enough to promote aggregation of these species in solution phase.

From a structural point of view, this study provided several key findings. First, the ditopic nature of the ligand does not have an influence over the coordination behavior of the individual $-PS_2$ groups: the structural features around the metallic center in these compounds are similar to those observed with "regular" monotopic dithiophosphonates. This observation suggests that using these or other polytopic dithiophosphonate ligands with different topologies in combination with various metallic centers we can expect to implement the observed rich coordination pattern of the $-PS_2$

groups (see Scheme 1) into the structural features of more complex polymetallic inorganic–organic hybrid materials.

A second important result of this work is that the different length of the ligand's side-arms is responsible for the different relative position of the –(An)PS_2**[M]** groups with respect to the central **NDI** moiety: in **1a-[$SnPh_3$]$_2$** and **1a-[Cu(PPh_3)$_2$]$_2$** they virtually surround the **NDI** group, while in **1b-[$SnPh_3$]$_2$** they are positioned away from the **NDI** moiety. This has a direct consequence on the supramolecular structures of these compounds. Comparing the supramolecular association of **1a-[$SnPh_3$]$_2$** with **1b-[$SnPh_3$]$_2$**, where the only difference between the compounds consist in the length of the side-arms, it can be easily observed that only in the case of **1a-[$SnPh_3$]$_2$** the **NDI** group is involved in the supramolecular architecture of the metal complex by participating in π–π stacking interactions with neighboring molecules. In the case of **{1a-[$SnPh_2$]}$_2$** and **1b-[$SnPh_2$]**, the same difference in the length of the linker also accounts for the mono/bimetallic composition of the macrocycles. The two side-arms of **1a** are not long enough to coordinate to only one metallic center, hence the need of two ligands and two tin centers for the formation of the macrocycle. In contrast, the length of the (–CH_2CH_2O–)$_2$ ether link in **1b** is sufficient to coordinate to one Ph_2Sn moiety. The consequence of these molecular structural features is the different supramolecular association of these compounds in solid state, where we note a change from infinite π–π stacked chains to discrete dimeric species.

3. Conclusions

A series of new metal complexes based on ligands having two dithiophosphonate donor groups linked to a 1,4,5,8-naphthalenediimide core through ether spacers of different length have been prepared and characterized in both solution and solid state. The crystal structures described above represent the first structurally characterized compounds consisting of metallic centers coordinated by ligands based on linking two dithiophosphonate groups within the same molecule. This study shows how changes in the length of the linker, while keeping the same donor set and topology of the ligand, can lead to different solid-state supramolecular architectures. We are currently exploring the potential of these ditopic dithiophosphonate ligands in the synthesis of novel supramolecular architectures using other metallic systems, capable of accommodating a greater number of –PS_2 donor groups. We are also investigating the use of other spacers to link two or more dithiophosphonate donor sets in the same ligand; these results will be reported in due course.

4. Experimental

4.1. General considerations

Unless otherwise noted, all operations were carried out in open air. Operations requiring inert (nitrogen) atmosphere were carried out using standard Schlenk techniques. Solvents were dried by conventional methods and distilled under a dry N_2 atmosphere immediately prior to use. Elemental analyses were performed by Robertson Microlit Laboratories, NJ. NMR spectra were recorded by using a 400 MHz Bruker Avance FT-NMR Spectrometer and a Varian Mercury/VX 400 Spectrometer. (Ph_3P)$_2$$CuNO_3$ was prepared according to published procedures [19]. All other reagents are commercially available (Sigma–Aldrich) and were used without further purification.

4.2. Synthesis of NDI-[CH_2CH_2OH]$_2$

A 250 mL flask was charged with a stirring bar, 1,4,5,8-naphthalenetetracarboxylic dianhydride (2.682 g, 0.01 mol) and 100 mL EtOH. To this mixture was added, under stirring, a solution of 2-aminoethanol (1.222 g, 0.02 mol) in 50 mL EtOH. The mixture was stirred overnight under reflux. After cooling at room temperature, the mixture was poured into 600 mL ice cold water and the resulting precipitate was filtered, washed with water (100 mL), ethanol (75 mL) and diethyl ether (75 mL), to afford the desired product (3.21 g, 90.6%) as a pink powder. ^{1}H NMR (400 MHz, DMSO-d_6): δ = 8.68 (s, 4H, *NDI*), 4.86 (t, J = 6.3 Hz, 2H, –O*H*), 4.18 (t, J = 6.2 Hz, 4H, –CH_2–), 3.68–3.65 (m, 4H, –CH_2–).

4.3. Synthesis of NDI-[$CH_2CH_2OCH_2CH_2OH$]$_2$

This compound was prepared as described above for **NDI-[CH_2-CH_2OH]$_2$**, using 1,4,5,8-naphthalenetetracarboxylic dianhydride (2.682 g, 0.01 mol) and 2-(2-aminoethoxy)ethanol (2.103 g, 0.02 mol). The compound (3.94 g, 89.1%) was isolated as a pale pink powder. ^{1}H NMR (400 MHz, DMSO-d_6): δ = 8.66 (s, 4H, *NDI*), 4.57 (t, J = 5.3 Hz, 2H, –O*H*), 4.27–4.25 (m, 4H, –CH_2–), 3.70–3.67 (m, 4H, –CH_2–), 3.49–3.46 (m, 8H, –CH_2–).

4.4. Synthesis of NDI-[CH_2CH_2O(An)PS_2NH_4]$_2$ (**1a-[NH_4]$_2$**)

Under a nitrogen atmosphere, a 250 mL flask was charged with a stirring bar, NDI-[CH_2CH_2OH]$_2$ (1.771 g, 5.0 mmol), 1,3,2,4-dithiadiphosphetane-2,4-bis(4-methoxyphenyl)-2,4-disulfide (Lawesson's Reagent, L.R.) (2.022 g, 5.0 mmol) and 150 mL dry benzene. The mixture was stirred under inert atmosphere for 90 min. at 80 °C, and allowed to cool at room temperature. Then, dry NH_3 gas (prepared from NH_4OH dropped onto solid NaOH and dried by passing it through a tower filled with powdered NaOH) was bubbled through the cold solution. The resulting voluminous precipitate was filtered, washed with cold benzene (50 mL) and then ether (2 × 50 mL) to afford an orange product (3.08 g, 77.7%), identified as NDI-[CH_2CH_2O(An)PS_2NH_4]$_2$···1/2 C_6H_6. ^{1}H NMR (400 MHz, Acetone-d_6/D_2O 5:0.6 v/v): δ = 8.67 (s, 4H, *NDI*), 7.85–7.82 (m, 4H, MeO–C_6H_4-P), 7.33 (s, 3H, C_6H_6), 6.45–6.42 (m, 4H, MeO–C_6H_4–P), 4.39 (t, J = 6.9 Hz, 4H, –CH_2–), 4.16–4.13 (m, 4H, –CH_2–), 3.58 (s, 6H, –O–CH_3); *Anal*. Calc. for $C_{35}H_{37}N_4O_8P_2S_4$: C, 50.53; H, 4.48; N, 6.73. Found: C, 50.26, H, 4.46, N, 6.69%.

4.5. Synthesis of NDI-[$CH_2CH_2OCH_2CH_2O$(An)PS_2NH_4]$_2$ (**1b-[NH_4]$_2$**)

This compound was prepared as described above for **1a-[NH_4]$_2$**, using NDI-[$CH_2CH_2OCH_2CH_2OH$]$_2$ (2.212 g, 5 mmol), L.R. (2.022 g, 5.0 mmol) and 150 mL benzene. The procedure afforded an orange product (3.28 g, 74.5%), identified as NDI-[$CH_2CH_2OCH_2CH_2$-O(An)PS_2NH_4]$_2$. ^{1}H NMR (400 MHz, Acetone-d_6/D_2O 5:0.6 v/v): δ = 8.72 (s, 4H, *NDI*), 7.97–7.94 (m, 4H, MeO–C_6H_4–P), 6.77–6.74 (m, 4H, MeO–C_6H_4–P), 4.36 (t, J = 6.8 Hz, 4H, –CH_2–), 3.92–3.89 (m, 4H, –CH_2–), 3.76–3.72 (m, 10H, 4H –CH_2– overlap with 6H –O–CH_3), 3.67–3.64 (m, 4H, –CH_2–); *Anal*. Calc. for $C_{36}H_{42}N_4O_{10}P_2S_4$: C, 49.08; H, 4.81; N, 6.36. Found: C, 48.82; H, 5.00; N, 6.20%.

4.6. Synthesis of NDI-[CH_2CH_2O(An)PS_2($SnPh_3$)$_2$]$_2$ (**1a-[$SnPh_3$]$_2$**)

A 250 mL flask was charged with a stirring bar and a solution of Ph_3SnCl (0.0964 g, 0.25 mmol) in DCM (75 mL). To this colorless solution was added, under vigorous stirring, an orange aqueous solution of **1a-[NH_4]$_2$** (0.0991 g, 0.125 mmol) in 75 mL water, and the mixture was stirred overnight. The completion of the reaction was indicated by the loss of the color of the aqueous phase and the appearance of an orange color in the organic phase. The organic phase was separated, and the aqueous phase extracted with DCM (3 × 10 mL). The combined organic phases were dried over anhydrous Na_2SO_4 and volatiles were removed under reduced pressure, to afford the title compound as an orange solid (0.1192 g, 65.5%).

^{1}H NMR (400 MHz, $CDCl_3$): δ = 8.58 (s, 4H, *NDI*), 7.60–7.52 (m, 16H, 4H MeO–C_6H_4–P overlap with 12H, Sn-(C_6H_5)$_3$), 7.37–7.33 (m, 18H, Sn-(C_6H_5)$_3$), 6.68–6.65 (m, 4H, MeO–C_6H_4–P), 4.51–4.47 (m, 4H, –CH_2–), 4.33–4.30 (m, 4H, –CH_2–), 3.76 (s, 6H, –O–CH_3). *Anal.* Calc. for $C_{68}H_{56}N_2O_8P_2S_4Sn_2$: C, 56.06; H, 3.87; N, 1.92. Found: C, 55.74, H, 3.69, N, 1.91%.

4.7. Synthesis of NDI-[CH_2CH_2O(An)PS_2(Cu(PPh_3)$_2$]$_2$ (**1a-[Cu(PPh_3)$_2$]$_2$**)

This compound was prepared as described above for **1a-[$SnPh_3$]$_2$**, using (Ph_3P)$_2$$CuNO_3$ (0.1625 g, 0.25 mmol) and **1a-[NH_4]$_2$** (0.0991 g, 0.125 mmol), to afford the title compound as a dark orange solid (0.1922 g, 79.5%). ^{1}H NMR (400 MHz, $CDCl_3$): δ = 8.59 (s, 4H, *NDI*), 7.78–7.75 (m, 4H, MeO–C_6H_4–P), 7.34–7.29 (m, 36H, –P(C_6H_5)$_3$), 7.19–7.16 (m, 24H, –P(C_6H_5)$_3$), 6.67–6.63 (m, 4H, MeO–C_6H_4–P), 4.47–4.45 (m, 4H, –CH_2–), 4.22–4.20 (m, 4H, –CH_2–), 3.73 (s, 6H, –O–CH_3). *Anal.* Calc. for $C_{104}H_{86}Cu_2N_2O_8P_6S_4$: C, 64.62; H, 4.48; N, 1.45. Found: C, 64.38; H, 4.35; N, 1.57%.

4.8. Synthesis of NDI-[$CH_2CH_2OCH_2CH_2O$(An)PS_2($SnPh_3$)$_2$]$_2$ (**1b-[$SnPh_3$]$_2$**)

A 250 mL flask was charged with a stirring bar and a solution of Ph_3SnCl (0.0964 g, 0.25 mmol) in DCM (75 mL). To this colorless solution was added, under vigorous stirring, an orange aqueous solution of **1b-[NH_4]$_2$** (0.110 g, 0.125 mmol) in 75 mL water, and the mixture was stirred overnight. The completion of the reaction was indicated by the loss of the color of the aqueous phase and the appearance of an orange color in the organic phase. The organic phase was separated, and the aqueous phase extracted with DCM (3 × 10 mL). The combined organic phases were dried over anhydrous Na_2SO_4 and volatiles were removed under reduced pressure, to afford the title compound as an orange solid (0.1427 g, 73.9%). ^{1}H NMR (400 MHz, $CDCl_3$): δ = 8.61 (s, 4H, *NDI*), 7.71–7.57 (m, 16H, 12H Sn–(C_6H_5)$_3$ overlap with 4H, MeO–C_6H_4–P), 7.42–7.39 (m, 18H, Sn–(C_6H_5)$_3$), 6.68–6.65 (m, 4H, MeO–C_6H_4–P), 4.43–4.41 (m, 4H, –CH_2–), 3.97–3.95 (m, 4H, –CH_2–), 3.82–3.76 (m, 10H, 6H, –O–CH_3 overlap with 4H, –CH_2–), 3.57–3.55 (m, 4H, –CH_2–). *Anal.* Calc. for $C_{72}H_{64}N_2O_{10}P_2S_4Sn_2$: C, 55.98; H, 4.18; N, 1.81. Found: C, 55.59; H, 3.90; N, 1.99%.

4.9. Synthesis of NDI-[$CH_2CH_2OCH_2CH_2O$(An)PS_2(Cu(PPh_3)$_2$]$_2$ (**1b-[Cu(PPh_3)$_2$]$_2$**)

This compound was prepared as described above for **1b-[$SnPh_3$]$_2$**, using (Ph_3P)$_2$$CuNO_3$ (0.1625 g, 0.25 mmol) and **1b-[NH_4]$_2$** (0.110 g, 0.125 mmol), to afford the title compound as a dark orange solid (0.2011 g, 79.6%). ^{1}H NMR (400 MHz, $CDCl_3$): δ = 8.57 (s, 4H, *NDI*), 7.66–7.64 (m, 4H, MeO–C_6H_4–P), 7.35–7.31 (m, 36H, –P(C_6H_5)$_3$), 7.24–7.22 (m, 24H, –P(C_6H_5)$_3$), 6.69–6.67 (m, 4H, MeO–C_6H_4–P), 4.48–4.45 (m, 4H, –CH_2–), 3.85–3.79 (m, 14H, 8H –CH_2– overlap with 6H –O–CH_3), 3.57–3.54 (m, 4H, –CH_2–). *Anal.* Calc. for $C_{108}H_{94}Cu_2N_2O_{10}P_6S_4$: C, 64.18; H, 4.69; N, 1.39. Found: C, 63.85; H, 4.34; N, 1.62%.

4.10. Synthesis of {NDI-[CH_2CH_2O(An)PS_2]$_2$($SnPh_2$)}$_2$ (**{1a-[$SnPh_2$]}$_2$**)

A 250 mL flask was charged with a stirring bar and a solution of Ph_2SnCl_2 (0.0429 g, 0.125 mmol) in DCM (75 mL). To this colorless solution was added, under vigorous stirring, an orange aqueous solution of **1a-[NH_4]$_2$** (0.0991 g, 0.125 mmol) in 75 mL water, and the mixture was stirred overnight. The completion of the reaction was indicated by the loss of the color of the aqueous phase and the appearance of an orange color in the organic phase. The organic phase was separated, and the aqueous phase extracted with DCM (3 × 10 mL). The combined organic phases were dried over anhydrous Na_2SO_4 and volatiles were removed under reduced pressure, to afford the title compound as an orange solid (0.1042 g, 80.9%). ^{1}H NMR (400 MHz, $CDCl_3$): δ = 8.57 (s, 8H, *NDI*), 7.71–7.68 (m, 8H, MeO–C_6H_4–P), 7.62–7.57 (m, 8H, Sn–(C_6H_5)$_3$), 7.51–7.48 (m, 12H, Sn–(C_6H_5)$_3$), 6.69–6.65 (m, 8H, MeO–C_6H_4–P), 4.48 (t, J = 5.7 Hz, 8H, –CH_2–), 4.33–4.28 (m, 8H, –CH_2–), 3.76 (s, 6H, –O–CH_3). *Anal.* Calc. for $C_{88}H_{72}N_4O_{16}P_4S_8Sn_2$: C, 51.32; H, 3.52; N, 2.72. Found: C, 51.56; H, 3.48; N, 2.89%.

4.11. Synthesis of NDI-[$CH_2CH_2OCH_2CH_2O$(An)PS_2]$_2$($SnPh_2$) (**1b-[$SnPh_2$]**)

This compound was prepared as described above for **{1a-[$SnPh_2$]}$_2$**, using Ph_2SnCl_2 (0.0429 g, 0.125 mmol) and **1b-[NH_4]$_2$** (0.110 g, 0.125 mmol) to afford the title compound as an orange solid (0. 1091 g, 78.1%). ^{1}H NMR (400 MHz, $CDCl_3$): δ = 8.59 (s, 4H, *NDI*), 7.61–7.59 (m, 4H, MeO–C_6H_4–P), 7.51–7.44 (m, 4H, Sn–(C_6H_5)$_3$), 7.35–7.30 (m, 6H, Sn–(C_6H_5)$_3$), 6.94–6.91 (m, 4H, MeO–C_6H_4–P), 4.42 (t, J = 4.7 Hz, 4H, –CH_2–), 3.99–3.97 (m, 4H, –CH_2–), 3.92 (s, 6H, –O–CH_3), 3.65–3.63 (m, 4H, –CH_2–), 3.54–3.52 (m, 4H, –CH_2–). *Anal.* Calc. for $C_{48}H_{44}N_2O_{10}P_2S_4Sn$: C, 51.58; H, 3.97; N, 2.51. Found: C, 51.36; H, 3.48; N, 2.72%.

4.12. Crystallographic studies

The X-ray data were collected at 100 K on a Bruker SMART APEXII CCD diffractomer equipped with Cu Kα radiation. Intensities were collected using phi and omega scans and were corrected for Lorentz polarizatrion and absorption effects. The *X-SEED* software platform [20], equipped with SHELXS and SHELXL modules on a PC computer [21], was used for all structure solution and refinement calculations and molecular graphics. The structure was solved by direct methods, and refined by anisotropic full-matrix least-squares for all non-hydrogen atoms. All hydrogen atoms were placed in calculated positions and refined using a riding model with fixed thermal parameters.

Acknowledgments

Acknowledgment is made to the Donors of the American Chemical Society Petroleum Research Fund for support of this research (grant 48039-GB3); the Single Crystal Diffractometer at EIU was purchased using funds provided by the NSF (CHE-0722547).

Appendix A. Supplementary material

CCDC 773639, 773642, 900068, 900069, and 900070 contain the supplementary crystallographic data for this paper. These data can be obtained free of charge from The Cambridge Crystallographic Data Centre via www.ccdc.cam.ac.uk/data_request/cif. Supplementary data associated with this article can be found, in the online version, at http://dx.doi.org/10.1016/j.ica.2013.02.037.

References

[1] (a) M. Yoshizawa, J.K. Klosterman, M. Fujita, Angew. Chem., Int. Ed. 48 (2009) 3418;
(b) Y. Inokuma, M. Kawano, M. Fujita, Nat. Chem. 3 (2011) 349;
(c) R. Chakrabarty, P.S. Mukherjee, P.J. Stang, Chem. Rev. 111 (2011) 6810;
(d) B.H. Northrop, Y.-R. Zheng, K.-W. Chi, P.J. Stang, Acc. Chem. Res. 42 (2009) 1554;
(e) G.F. Swiegers, T.J. Malefetse, Chem. Rev. 100 (2000) 3483;
(f) L. Brammer, Chem. Soc. Rev. 33 (2004) 476;
(g) H.-B. Yang, K. Ghosh, B.H. Northrop, P.J. Stang, Org. Lett. 9 (2007) 1561;
(h) A. Sautter, D.G. Schmid, G. Jung, J. Am. Chem. Soc. 123 (2001) 5424;
(i) D. Schultz, J.R. Nitschke, Angew. Chem. 118 (2006) 2513.

[2] (a) M. Albrecht, Chem. Rev. 101 (2001) 3457;
(b) M. Albrecht, Chem. Soc. Rev. 27 (1998) 281.
[3] (a) K.M.-C. Wong, V.W.-W. Yam, Acc. Chem. Res. 44 (2011) 424;
(b) V.W.-W. Yam, K.M.-C. Wong, Chem. Commun. 47 (2011) 11579.
[4] (a) C. Pettinari, R. Pettinari, Coord. Chem. Rev. 249 (2005) 525;
(b) C. Pettinari, R. Pettinari, Coord. Chem. Rev. 249 (2005) 663.
[5] (a) I. Haiduc, D.B. Sowerby, S.F. Lu, Polyhedron 14 (1995) 3389;
(b) I. Haiduc, D.B. Sowerby, Polyhedron 15 (1996) 2469;
(c) I. Haiduc, in: F. Devillanova (Ed.), Handbook of Chalcogen Chemistry. New Perspectives in Sulfur, Selenium and Tellurium, RSC Publishing, The Royal Society of Chemistry, London, 2007, pp. 593–643;
(d) E.R.T. Tiekink, J. Zukerman-Schpector, Coord. Chem. Rev. 254 (2010) 46;
(e) E.R.T. Tiekink, CrystEngComm 8 (2006) 104;
(f) E.R.T. Tiekink, Met. Chem. 15 (1992) 161.
[6] (a) M.E. Padilla-Tosta, O.D. Fox, M.G.B. Drew, P.D. Beer, Angew. Chem., Int. Ed. 40 (2001) 4235;
(b) P.D. Beer, N. Berry, M.G.B. Drew, O.D. Fox, M.E. Padilla-Tosta, S. Patell, Chem. Commun. (2001) 199;
(c) P.D. Beer, A.G. Cheetham, M.G.B. Drew, O.D. Fox, E.J. Hayes, T.D. Rolls, Dalton Trans. (2003) 603;
(d) W.W.H. Wong, D. Curiel, A.R. Cowley, P.D. Beer, Dalton Trans. (2005) 359;
(e) W.W.H. Wong, D. Curiel, S.-W. Lai, M.G.B. Drew, P.D. Beer, Dalton Trans. (2005) 774;
(f) J. Cookson, P.D. Beer, Dalton Trans. (2007) 1459.
[7] (a) M.J. Macgregor, G. Hogarth, A.L. Thompson, J.D.E.T. Wilton-Ely, Organometallics 28 (2009) 197;
(b) S. Naeem, A.J.P. White, G. Hogarth, J.D.E.T. Wilton-Ely, Organometallics 29 (2010) 2547.
[8] R. Reyes-Martínez, P. García y García, M. López-Cardoso, H. Höpfl, H. Tlahuext, Dalton Trans. (2008) 6624.
[9] (a) M.C. Aragoni, M. Arca, N.R. Champness, A.V. Chernikov, F.A. Devillanova, F. Isaia, V. Lippolis, N.S. Oxtoby, G. Verani, S.Z. Vatsadze, C. Wilson, Eur. J. Inorg. Chem. (2004) 2008;
(b) M.C. Aragoni, M. Arca, M. Crespo, F.A. Devillanova, M.B. Hursthouse, S.L. Huth, F. Isaia, V. Lippolis, G. Verani, CrystEngComm 9 (2007) 873;
(c) M.C. Aragoni, M. Arca, M. Crespo, F.A. Devillanova, M.B. Hursthouse, S.L. Huth, F. Isaia, V. Lippolis, G. Verani, Dalton Trans. (2009) 2510.
[10] (a) M. Karakus, H. Yilmaz, E. Bulak, Russ. J. Coord. Chem. 31 (2005) 316;
(b) A.R. Gataulina, D.A. Safin, T.R. Gimadiev, M.V. Pinus, Transition Met. Chem. 33 (2008) 921.
[11] (a) A. Bondi, J. Phys. Chem. 68 (1964) 441;
(b) R.S. Rowland, R. Taylor, J. Phys. Chem. 100 (1996) 7384.
[12] (a) N.W. Alcock, Adv. Inorg. Chem. Radiochem. 15 (1972) 1;
(b) N.W. Alcock, R.M. Countryman, J. Chem. Soc., Dalton Trans. (1977) 217;
(c) I. Haiduc, Appl. Organomet. Chem. 21 (2007) 476;
(d) I. Haiduc, Coord. Chem. Rev. 158 (1997) 325;
(e) E.R.T. Tiekink, CrystEngComm 5 (2003) 101.
[13] (a) C.A. Hunter, J.K.M. Sanders, J. Am. Chem. Soc. 120 (1990) 5525;
(b) C. Janiak, J. Chem. Soc., Dalton Trans. (2000) 3885 (and references therein).
[14] (a) M. Nishio, M. Hirota, Y. Umezawa, The CH/π Interaction: Evidence, Nature and Consequences, Wiley–VCH, New-York, 1998;
(b) W.B. Jennings, B.M. Farrell, J.F. Malone, Acc. Chem. Res. 34 (2001) 885;
(c) M. Nishio, CrystEngComm 6 (2004) 130.
[15] (a) I.G. Dance, M.L. Scudder, J. Chem. Soc., Chem. Commun. (1995) 1039;
(b) I.G. Dance, M.L. Scudder, J. Chem. Soc., Dalton Trans. (1998) 1341;
(c) V. Russel, M.L. Scudder, I.G. Dance, J. Chem. Soc., Dalton Trans. (2001) 789;
(d) I.G. Dance, CrystEngComm 5 (2003) 208.
[16] (a) D.G. Hamilton, J.E. Davies, L. Prodi, J.K.M. Sanders, Chem. Eur. J. 4 (1998) 608;
(b) D.G. Hamilton, M. Montalti, L. Prodi, M. Fontani, P. Zanello, J.K.M. Sanders, Chem. Eur. J. 6 (2000) 608.
[17] P.S. Pregosin, P.G.A. Kumar, I. Fernandez, Chem. Rev. 105 (2005) 2977 (and references therein).
[18] (a) J. Fielden, D. Long, A.M.Z. Slawin, P. Ko1gerler, L. Cronin, Inorg. Chem. 46 (2007) 9090;
(b) G. Consiglio, S. Failla, P. Finocchiaro, I.P. Oliveri, R. Purrello, S.D. Bella, Inorg. Chem. 49 (2010) 5134.
[19] F.A. Cotton, D.M.L. Goodgame, J. Chem. Soc. (1960) 5267.
[20] L.J. Barbour, Supramol. Chem. 1 (2001) 189.
[21] G.M. Sheldrick, Acta Crystallogr., Sect. A 64 (2008) 112.